A NEW APPROACH FOR HEART RATE MONITORING USING PHOTOPLETHYSMOGRAPHY SIGNALS CONTAMINATED BY MOTION ARTIFACTS

*Biao Sun**, *Hui Feng*

Tianjin University
School of Electrical Engineering and Automation
Tianjin, 300072, China

Zhilin Zhang

Samsung Research America
Dallas, 1301 East Lookout Drive
Richardson, TX 75082.

ABSTRACT

We considered the problem of accurately estimating the heart rate (HR) using photoplethysmography (PPG) signals that are contaminated by motion artifacts (MA). A novel HR estimation approach based on GRidless spectral Estimation and SVM-based peak Selection, denoted by GRESS, was proposed. It first obtained the sparse spectrum of PPG using a continuous dictionary, then a simple spectral subtraction step was adopted to remove MA, finally an SVM-based method was developed to select the spectral peak corresponding to HR. Experimental results on the PPG datasets used in 2015 IEEE Signal Processing Cup showed that the proposed approach had excellent performance. The average absolute error on 12 training sets was 1.45 beat per minute (BPM) (standard deviation: 2.21 BPM). The average absolute error on the 10 testing sets was 1.78 BPM (standard deviation: 3.07 BPM).

Index Terms— Photoplethysmography (PPG), heart rate, motion artifacts, gridless spectral estimation, SVM

1. INTRODUCTION

Heart Rate (HR) measurement is one of the most important approaches for exercisers to monitor cardiac status and control their training load. Conventional HR measurement techniques such as ECG were limited in their high hardware complexity and low user comfortability. Photoplethysmography (PPG) is a non-invasive and low cost tool to monitor blood volume changes in tissue continuously. Motivated by its efficiency and easy integration, PPG powers many aspects of modern society: from personal-Health to clinical physiological monitoring, and it is increasingly present in consumer products such as wearable devices and smartphones [1, 2]. However, the main disadvantage of PPG is that the quality of the signals can be easily influenced by motion artifacts (MA) [3]. During subjects' intensive exercises, MA are more frequent and can become a serious obstacle to the reliable use of PPG.

To enhance the signal quality in the presence of MA, various approaches such as blind source separation (BSS) [4], adaptive noise cancellation (ANC) [5], empirical mode decomposition (EMD) technique [6], spectral subtraction method [7], and wavelet-based method [8], have been investigated. Recently, Zhang *et al.* proposed a novel method named TROIKA [9] , and its variant JOSS [10] to monitor HR using PPG. They can be seen as the state-of-the-art due to their high performance. However, these methods had two main drawbacks. For one thing, TROIKA and JOSS assumed that PPG can be sparsely represented under a redundant discrete Fourier transform (DFT) basis, i.e., the continuous frequency domain was discretized into a finite set of grid points. Then the spectrum of PPG were estimated using an sparse signal recovery (SSR) algorithm. Nevertheless, like most natural signals, the sparsity of PPG spectrum is not generally aligned with any frequency grid. Consequently, recovering the 'off-the-grid' PPG spectrum with a discrete basis will cause the 'basis mismatch' problem [11], whereby even a good signal model may bring out a poor representation due to seemingly small differences between basis vectors and a similar set yielding a far sparser representation of the signal [12]. For another, TROIKA and JOSS required careful engineering and considerable expertise to adjust reliable parameters and to design a spectral peak selector that find out the peaks corresponding to HR. Therefore, these methods had low generalization ability and performed poorly on new PPG signals with heavy MA.

To develop an effective HR estimation method using PPG corrupted by MA, a novel approach termed GRESS was proposed in this paper. Firstly, the PPG spectrum was estimated using a grid-less spectral estimation method. Secondly, a simple but effective spectral subtraction step was adopted to remove MA, largely reducing false spectral peaks and making PPG spectrum cleaner. Finally, an SVM-based method was proposed to select the spectral peak corresponding to HR.

The main contributions of the work are as follows.

1) Instead of using conventional grid spectral estimation methods, a grid-less alternative was developed to estimate PPG spectrum, overcoming the basis mismatch problem and increasing the estimation accuracy.

2) The spectral peak selection problem is formulated into a pattern classification task, and an SVM-based approach was used to find the spectral peaks corresponding to HR. To the best of our knowledge, most existing algorithms [9, 10] used heuristic methods to find the spectral peaks corresponding to HR, which involve many user-tuning parameters. Compared to heuristic methods, the proposed approach gave GRESS better generalization ability and robustness on new datasets.

2. METHOD

The proposed method estimated HR using a raw PPG signal and a simultaneous tri-axis acceleration signal. A time window with length of 8 seconds and overlap of 2 seconds was used to slide the simultaneous PPG and acceleration signals, and HR was estimated in the time window. A pre-processing step was adopted that PPG and acceleration signals were processed by a bandpass filter with a low cut-off frequency and a high cut-off frequency of 0.5 Hz and 4.0

*This work was supported by the National Natural Science Foundation of China under Grants 61271321, 61473207 and 61401303.

Hz, respectively. After that, HR were estimated by GRESS. The flowchart of GRESS is depicted in Fig 1.

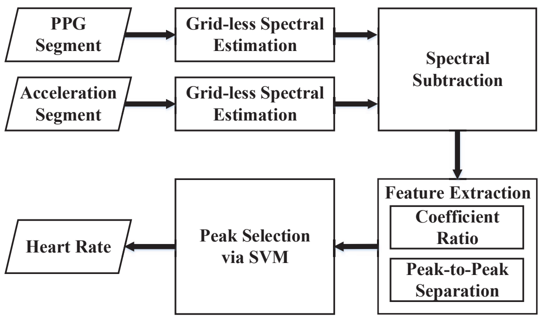

Fig. 1. Flowchart of GRESS.

2.1. Grid-less Spectral Estimation

In this paper, the spectrum of PPG signal was assumed to be sparse, i.e., a segment of raw PPG signal $\boldsymbol{x} \in \mathbb{C}^{N\times 1}$ can be expressed as

$$\boldsymbol{x} = \sum_{k=1}^{K} c_k a(f_k) + \boldsymbol{e} = \boldsymbol{A}(\boldsymbol{f})\boldsymbol{c} + \boldsymbol{e}, \tag{1}$$

where K is the sparsity level, $\boldsymbol{c} \in \mathbb{C}^{N\times 1}$ is the coefficients vector, $\boldsymbol{e} \in \mathbb{C}^{N\times 1}$ is the measurement noise, $a(f_k) \in \mathbb{C}^{N\times 1}$ is the atom defined as $a(f_k) = e^{i2\pi f_k}$, and $\boldsymbol{A}(\boldsymbol{f}) = [a(f_1), \ldots, a(f_K)] \in \mathbb{C}^{N\times K}$. In the presence of independently and identically distributed zero-mean Gaussian noise with variance σ_0, the noiseless PPG signal $\boldsymbol{z} = \boldsymbol{A}(\boldsymbol{f})\boldsymbol{c}$ can be estimated using the atomic norm soft thresholding (AST) method [13], which tried to solve the following optimization problem

$$\underset{\boldsymbol{z}}{\operatorname{argmin}} \frac{1}{2}\|\boldsymbol{x} - \boldsymbol{z}\|_2^2 + \tau\|\boldsymbol{z}\|_{\mathcal{A}}, \tag{2}$$

where τ is an appropriately chosen regularization parameter. $\mathcal{A}$ is the spectral atomic set defined as

$$\mathcal{A} = \{a(f) : f \in [0, 1]\}, \tag{3}$$

and $\|\boldsymbol{z}\|_{\mathcal{A}}$ is the atomic norm of $\boldsymbol{z}$ defined as

$$\|\boldsymbol{z}\|_{\mathcal{A}} = \inf\left\{\sum_k c_k : \boldsymbol{z} = \sum_k c_k a(f_k).\right\} \tag{4}$$

The problem (2) can be computed via semidefinite programming (SDP) [13]:

$$\underset{t,\boldsymbol{u},\boldsymbol{z}}{\operatorname{argmin}} \frac{1}{2}\|\boldsymbol{x} - \boldsymbol{z}\|_2^2 + \frac{\tau}{2}(t + u_1), \text{ s.t. } \begin{bmatrix} t & \boldsymbol{z}^H \\ \boldsymbol{z} & T(\boldsymbol{u}) \end{bmatrix} \geq 0, \tag{5}$$

where $\boldsymbol{u} \in \mathbb{C}^N$ and $T(\boldsymbol{u}) \in \mathbb{C}^{N\times N}$ denotes a (Hermitian) Toeplitz matrix with

$$T(\boldsymbol{u}) = \begin{bmatrix} u_1 & u_2 & \ldots & u_N \\ u_2^{\mathrm{H}} & u_1 & \ldots & u_{N-1} \\ \vdots & \vdots & \ddots & \vdots \\ u_N^{\mathrm{H}} & u_{N-1}^{\mathrm{H}} & \ldots & u_1 \end{bmatrix}, \tag{6}$$

where u_j denotes the jth entry of $\boldsymbol{u}$. The SDP problem (5) can be solved efficiently by the Alternating Direction Method of Multipliers (ADMM) based algorithm [13]. Given the optimal solution $(t^*, \boldsymbol{u}^*, \boldsymbol{z}^*)$, the frequency and coefficient estimates $\hat{\boldsymbol{f}}$ and $\hat{\boldsymbol{c}}$ can be obtained via Vandermonde decomposition of $T(\boldsymbol{u}^*)$ [14],

$$T(\boldsymbol{u}^*) = \boldsymbol{A}\left(\hat{\boldsymbol{f}}, \hat{\boldsymbol{\phi}}\right) \cdot \operatorname{diag}(|\hat{\boldsymbol{c}}|) \cdot A^{\mathrm{H}}\left(\hat{\boldsymbol{f}}, \hat{\boldsymbol{\phi}}\right). \tag{7}$$

Using the grid-less spectral estimation method described above, both spectra of PPG and acceleration signals can be estimated accurately.

2.2. Spectral Subtraction

Inspired by our knowledge that the spectral components of MA in PPG are correlated to those of the acceleration signal, a spectral subtraction algorithm was proposed to remove MA from PPG. However, Due to the fact that the spectrum was estimated in continuous setting, the spectral lines of PPG and those of acceleration signal may not fall in the same positions exactly. To simplify the subtraction procedure, a tolerant parameter $\sigma > 0$ was introduced to measure the similarity of two spectral lines. Only if the distance between a spectral line of PPG and that of acceleration signal is less than σ, the subtraction will be executed. The pseudo-code is depicted in Algorithm 1, where $(\boldsymbol{f}^{\text{PPG}}, \boldsymbol{c}^{\text{PPG}}), (\boldsymbol{f}^{\text{ACC}}, \boldsymbol{c}^{\text{ACC}}), \left(\boldsymbol{f}^{\text{CLN}}, \boldsymbol{c}^{\text{CLN}}\right)$ denote the frequencies and coefficients of PPG, acceleration signals, and cleansed PPG, respectively. $k1$ and $k2$ denote the sparsity levels of PPG spectrum and acceleration spectrum, respectively. To ensure the spectral subtraction method effective, each of the PPG segments and acceleration segments should be normalized to have the same energy.

Algorithm 1 Spectral Subtraction

Input: $(\boldsymbol{f}^{\text{PPG}}, \boldsymbol{c}^{\text{PPG}}), (\boldsymbol{f}^{\text{ACC}}, \boldsymbol{c}^{\text{ACC}}), \sigma$;
for each $i \in 1, \ldots, k1$ **do**
  $f_i^{\text{CLN}} = f_i^{\text{PPG}}, \quad c_i^{\text{CLN}} = c_i^{\text{PPG}}$
  for each $j \in 1, \ldots, k2$ **do**
    if $|f_i^{\text{PPG}} - f_j^{\text{ACC}}| < \sigma$ **then**
      $c_i^{\text{CLN}} = c_i^{\text{PPG}} - c_j^{\text{ACC}}$
    end if
  end for
end for
Output: cleansed PPG spectrum $\left(\boldsymbol{f}^{\text{CLN}}, \boldsymbol{c}^{\text{CLN}}\right)$

2.3. SVM-based Spectral Peak Selection

Given the cleansed PPG spectrum $\left(\boldsymbol{f}^{\text{CLN}}, \boldsymbol{c}^{\text{CLN}}\right)$, an candidate spectral peak set Ω is formed using a hard thresholding method, i.e.,

$$\Omega = \left\{\left(f_i^{\Omega}, c_i^{\Omega}\right) : c_i^{\Omega} > \delta * c_{\max}^{\text{CLN}}\right\}, \tag{8}$$

where $c_{\max}^{\text{CLN}}$ is the maximum value of c^{CLN} and δ is a threshold factor. Then a peak selection algorithm is proposed to find out the best reliable spectral peak in the candidate peak set. This task can be considered as a type of two-category classification problem, i.e., divide candidate peaks into two classes: true peak (there is only one true peak in each time window) and false peaks. Based on our observations on available PPG data, true spectral peaks corresponding to HR are observed to have noticeably different coefficients when compared to false peaks. Moreover, the peak-to-peak separation of true peaks differ from those of false peaks. Therefore, amplitude ratio and peak-to-peak separation are considered as features to quantify differences among the candidate spectral peaks.

Suppose there are p peaks in the candidate peak set Ω, the *coefficient ratio* of the i^{th} candidate peak, denoted by R_i, is defined as

$$R_i = \left| \frac{c_i}{c_{\text{max}}^{\Omega}} \right|, \quad i = 1, \ldots, p, \quad R_i \in (0, 1], \tag{9}$$

where c_i is coefficient of the i^{th} candidate peak and c_{max}^{Ω} is the maximum coefficient in Ω. The *peak-to-peak separation* of the i^{th} candidate peak, denoted by S_i, is defined as

$$S_i = |f_i - f_{\text{pre}}|, \tag{10}$$

where f_i is the frequency of the i^{th} candidate peak and f_{pre} is the true peak in previous time window.

Based on the two features described above, we adopted *Support Vector Machine* (SVM)[15] to build a decision boundary classifying true spectral peaks from false ones. SVM is widely used in classification and regression due to its accuracy and robustness to noise. The SVM-based spectral peak selection method consists of training and test phases. The two features are firstly extracted from all candidate peaks which are labeled separately. The true peaks are labeled as '1' while the false peaks are labeled as '0'. The SVM then trains itself with the labeled features and finds the support vectors among the features which maximize the margin (or the distance) between different classes. Finally, the SVM builds a decision boundary from the support vectors. Noting that some candidate peaks are mixed and cannot be separated, we consider using a soft-margin SVM [16] to set the boundary.

Given a trained SVM classifier, the true peak can be found as follows. We first extract the two features of candidate peaks and construct feature vectors, then examine whether they are true peaks by trained SVM classifier. It is worth noting that classifier may select no peak or more than one peak as true in the time window. Therefore, we choose the peak corresponding to HR, denoted by f_{HR}, as follows,

1. Only one peak is classified as true, then we choose the peak as f_{HR}.
2. More than one peak is classified as true, then we choose the peak which is closest to f_{pre} as f_{HR}, i.e.,

$$f_{\text{HR}} = \min_{f_i} |f_i - f_{\text{pre}}|\,. \tag{11}$$

3. No peak is classified as true. In this situation, we reach the conclusion that the current PPG segment is seriously corrupted, and SVM cannot find reliable peaks. Therefore we discard the segment by assigning $f_{\text{HR}} = f_{\text{pre}}$.

Once an f_{HR} is decided, the estimated HR in current window is computed via

$$\text{BPM}_{\text{est}} = f_{\text{HR}} * 60. \tag{12}$$

3. EXPERIMENTAL RESULTS

3.1. Experimental Setup

The PPG database was used for the 2015 IEEE Signal Processing Cup. It includes 12 training datasets and 10 test datasets. Each dataset consists of two channels of PPG signals, three channels of simultaneous acceleration signals, and one channel of simultaneous ECG signal. The PPG signals were recorded from subjects' wrist (dorsal locations) using PPG sensors built in a wristband. The PPG sensors used green LEDs working at 515 nm. The acceleration signals were recorded using a tri-axis accelerometer also built in the wristband. The ECG signals were recorded using wet ECG sensors locating at the chest of subjects. The ground-truth of heart rate was calculated from the ECG signal, which was used to evaluate algorithms' performance. All signals were sampled at 125 Hz.

Three measurement indexes were used to evaluate the performance of GRESS. The first measurement index was the average absolute error (in BPM), defined as

$$\text{Error1} = \frac{1}{\text{D}} \sum_{\text{i}=1}^{\text{D}} |\text{BPM}_{\text{est}}(\text{i}) - \text{BPM}_{\text{ECG}}(\text{i})|\,, \tag{13}$$

where D is the total number of time windows, $\text{BPM}_{\text{ECG}}(i)$ the ground-truth of HR in the i^{th} time window calculated from the simultaneously recorded ECG signal, and $\text{BPM}_{\text{est}}(i)$ the estimated HR using GRESS.

The second was the average absolute error percentage, defined as

$$\text{Error2} = \frac{1}{\text{D}} \sum_{\text{i}=1}^{\text{D}} \frac{|\text{BPM}_{\text{est}}(\text{i}) - \text{BPM}_{\text{ECG}}(\text{i})|}{\text{BPM}_{\text{ECG}}(\text{i})}. \tag{14}$$

As the third measurement index, Bland–Altman plots [17, 18] were used for combined graphical and statistical interpretation of the two measurement techniques. The differences between heart rate measurements from the wrist and ECG were expressed as percentages of the averages in both techniques and plotted against the averages. The 95% Limit of Agreement (LOA) was calculated in this analysis, which is defined as the average absolute error ± 1.96 standard deviation of the absolute error $([\mu_{\text{E}} - 1.96\sigma_{\text{E}}, \mu_{\text{E}} + 1.96\sigma_{\text{E}}])$.

The training datasets were used to train the SVM classifier. After that all training datasets and test datasets were used to evaluate the performance of GRESS.

3.2. Results

To evaluate the performance of GRESS, we compared it with TROIKA and JOSS, which can be seen as the state-of-the-art. The average absolute error (Error1) and the average absolute error percentage (Error2) on the 12 training datasets are given in Table 1 and Table 2. It can be seen that GRESS had better performance than

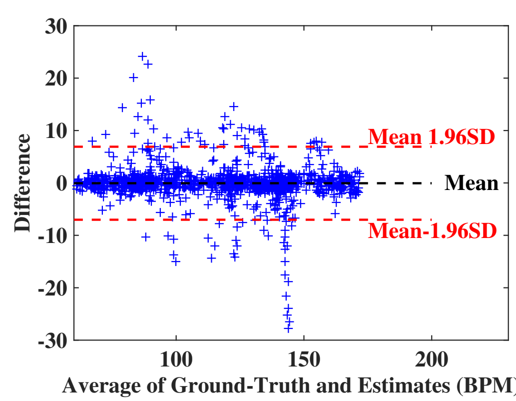

Fig. 2. The Bland-Altman plot of the estimation results over all 22 datasets. The LOA is [-7.02, 6.90] BPM.

Table 1. Comparision of GRESS, TROIKA and JOSS in terms of average absolute error (Error1) on the 12 training datasets. The unit is BPM. SD indicates the standard deviation.

	No.1	No.2	No.3	No.4	No.5	No.6	No.7	No.8	No.9	No.10	No.11	No.12	**Average**
GRESS	1.18	2.42	0.86	1.38	0.76	1.37	0.72	0.64	0.60	3.65	0.82	1.04	**1.45 (SD=2.21)**
TROIKA	2.87	2.75	1.91	2.25	1.69	3.16	1.72	1.83	1.58	4.00	1.96	3.33	**2.42 (SD=2.47)**
JOSS	1.33	1.75	1.47	1.48	0.69	1.32	0.71	0.56	0.49	3.81	0.78	1.04	**1.28 (SD=2.61)**

Table 2. Comparision of GRESS, TROIKA and JOSS in terms of average absolute error percentage (Error2) on the 12 training datasets. The unit is percentage (%). SD indicates the standard deviation.

	No.1	No.2	No.3	No.4	No.5	No.6	No.7	No.8	No.9	No.10	No.11	No.12	**Average**
GRESS	1.02	2.30	0.76	1.31	0.77	1.15	1.26	0.54	0.52	2.31	0.75	0.91	**1.21 (SD=1.56)**
TROIKA	2.18	2.37	1.50	2.00	1.22	2.51	1.27	1.47	1.28	2.49	1.29	2.30	**1.82 (SD=2.07)**
JOSS	1.19	1.66	1.27	1.41	0.51	1.09	0.54	0.47	0.41	2.43	0.51	0.81	**1.01 (SD=2.29)**

Table 3. The Error1 and Error2 of GRESS on the 10 test datasets. The units of Error1 and Error2 are BPM and percentage (%), respectively. SD indicates the standard deviation.

	No.1	No.2	No.3	No.4	No.5	No.6	No.7	No.8	No.9	No.10	**Average**
Error1	5.63	1.23	1.75	1.29	1.89	2.62	2.24	2.31	0.94	0.61	**1.78 (SD=3.07)**
Error2	6.51	1.51	1.44	0.82	1.59	1.95	2.46	1.68	0.74	0.71	**1.57 (SD=2.71)**

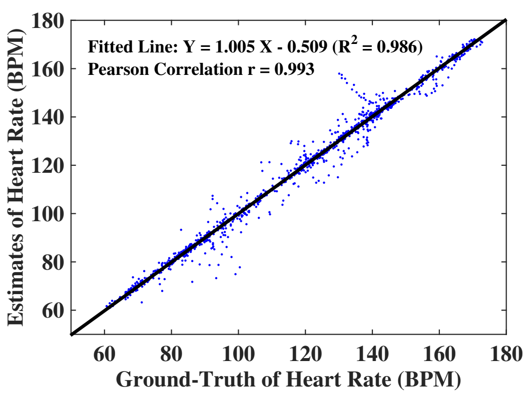

Fig. 3. Scatter plot between the ground-truth heart rate values and the associated estimates over all 22 datasets.

TROIKA. Although GRESS had a larger average error than JOSS, the smaller standard deviation implied that GRESS had better robustness and generalization ability than JOSS. In addition, averaged across the 12 RAD, the Error1 of GRESS was 1.45 ± 2.21 BPM (mean $\pm$ standard deviation), and the error percentage (Error2) was $1.21\% \pm 1.56\%$. In contrast, TROIKA had the performance of Error1 = 2.42 ± 2.47 BPM and Error2 = $1.82\% \pm 2.07\%$. JOSS had the performance of Error1 = 1.28 ± 2.61 BPM and Error2 = $1.01\% \pm 2.29\%$ (These results were directly adopted from [9] and [10]).

We further evaluated the performance of GRESS on the 10 test datasets. The average absolute error (Error1) and the average absolute error percentage (Error2) are given in Table 3. Averaged across the 10 test datasets, the Error1 of GRESS was 1.78 ± 3.07 BPM, and the Error2 was $1.57\% \pm 2.71\%$. Note that these results were much better than that of the first place in the 2015 IEEE Signal Processing Cup[1].

The Bland-Altman plot over all 22 datasets is depicted in Figure 2, where the LOA was [-7.02, 6.90] BPM. The Scatter Plot between the ground-truth HR values and the associated estimates is given in Figure 3, which shows the fitted line was $Y = 1.005X - 0.509$, where X indicates the ground-truth heart rate value, and Y indicates the associated estimate. The Pearson coefficient was 0.993. The goodness of fit characterized by R^2 value was 0.986.

4. CONCLUSIONS

We have presented a new method termed GRESS for HR estimation using a wrist-type PPG during physical exercise which is based on the grid-less spectrum estimation and SVM-based peak selection. Experimental results proved the efficacy of GRESS for reliable and accurate estimation of heart rate.

5. REFERENCES

[1] John Allen, "Photoplethysmography and its application in clinical physiological measurement," *Physiological measurement*, vol. 28, no. 3, pp. R1–R39, 2007.

[2] K Nakajima, T Tamura, and H Miike, "Monitoring of heart and respiratory rates by photoplethysmography using a digital filtering technique," *Medical engineering & physics*, vol. 18, no. 5, pp. 365–372, 1996.

[1] The average absolute error (over the testing datasets) of the first three places in the Cup were 2.27 BPM, 3.26 BPM, and 3.44 BPM, respectively. (http://www.signalprocessingsociety.org/spcup2015/.)

[3] R Sahni, A Gupta, K Ohira-Kist, and TS Rosen, "Motion resistant pulse oximetry in neonates," *Archives of Disease in Childhood-Fetal and Neonatal Edition*, vol. 88, no. 6, pp. F505–F508, 2003.

[4] Byung S Kim and Sun K Yoo, "Motion artifact reduction in photoplethysmography using independent component analysis," *Biomedical Engineering, IEEE Transactions on*, vol. 53, no. 3, pp. 566–568, 2006.

[5] JM Graybeal and MT Petterson, "Adaptive filtering and alternative calculations revolutionizes pulse oximetry sensitivity and specificity during motion and low perfusion," in *Engineering in Medicine and Biology Society, 2004. IEMBS'04. 26th Annual International Conference of the IEEE*. IEEE, 2004, vol. 2, pp. 5363–5366.

[6] Xuxue Sun, Ping Yang, Yulin Li, Zhifan Gao, and Yuan-Ting Zhang, "Robust heart beat detection from photoplethysmography interlaced with motion artifacts based on empirical mode decomposition," in *Biomedical and Health Informatics (BHI), 2012 IEEE-EMBS International Conference on*. IEEE, 2012, pp. 775–778.

[7] B. Sun and Z. Zhang, "Photoplethysmography-based heart rate monitoring using asymmetric least squares spectrum subtraction and bayesian decision theory," *Sensors Journal, IEEE*, 2015, DOI 10.1109/JSEN.2015.2473697.

[8] CM Lee and YT Zhang, "Reduction of motion artifacts from photoplethysmographic recordings using a wavelet denoising approach," in *Biomedical Engineering, 2003. IEEE EMBS Asian-Pacific Conference on*. IEEE, 2003, pp. 194–195.

[9] Zhilin Zhang, Zhouyue Pi, and Benyuan Liu, "Troika: A general framework for heart rate monitoring using wrist-type photoplethysmographic signals during intensive physical exercise," *Biomedical Engineering, IEEE Transactions on*, vol. 62, no. 2, pp. 522–531, 2015.

[10] Zhilin Zhang, "Photoplethysmography-based heart rate monitoring in physical activities via joint sparse spectrum reconstruction," *Biomedical Engineering, IEEE Transactions on*, vol. 62, no. 8, pp. 1902–1910, Aug 2015.

[11] Yuejie Chi, Louis L Scharf, Ali Pezeshki, and A Robert Calderbank, "Sensitivity to basis mismatch in compressed sensing," *Signal Processing, IEEE Transactions on*, vol. 59, no. 5, pp. 2182–2195, 2011.

[12] Gongguo Tang, Badri Narayan Bhaskar, Parikshit Shah, and Benjamin Recht, "Compressed sensing off the grid," *Information Theory, IEEE Transactions on*, vol. 59, no. 11, pp. 7465–7490, 2013.

[13] Badri Narayan Bhaskar, Gongguo Tang, and Benjamin Recht, "Atomic norm denoising with applications to line spectral estimation," *Signal Processing, IEEE Transactions on*, vol. 61, no. 23, pp. 5987–5999, 2013.

[14] Zai Yang and Lihua Xie, "On gridless sparse methods for line spectral estimation from complete and incomplete data," *Signal Processing, IEEE Transactions on*, vol. 63, no. 12, pp. 3139–3153, June 2015.

[15] Corinna Cortes and Vladimir Vapnik, "Support-vector networks," *Machine learning*, vol. 20, no. 3, pp. 273–297, 1995.

[16] Chih-Wei Hsu, Chih-Chung Chang, Chih-Jen Lin, et al., "A practical guide to support vector classification," 2003.

[17] J Martin Bland and DouglasG Altman, "Statistical methods for assessing agreement between two methods of clinical measurement," *The lancet*, vol. 327, no. 8476, pp. 307–310, 1986.

[18] J Martin Bland and Douglas G Altman, "Agreement between methods of measurement with multiple observations per individual," *Journal of biopharmaceutical statistics*, vol. 17, no. 4, pp. 571–582, 2007.